Using Of Artificial Neural Network For Modeling Of Oily Wastewater In Reverse Osmosis Process

Mansoor Kazemimoghadam

Malek Ashtar University of Technology, Tehran, Iran,
mzkazemi@gmail.com

Abstract: Primary reason for flux decline during the initial period of a membrane separation process is concentration polarization of solute at the membrane surface. This can occur in conjunction with irreversible fouling of the membrane as well as reversible gel/cake layer formation. Oily water emulsions are one of the main pollutants emitted into water by industries and domestic sewage. Also, oily water in inland waterways and coastal zone is one of the most serious issues of water pollution which needs to be resolved urgently. The results of an experimental study on separation of oil from oily waters are presented. A Film Tec FT30 membrane as a reverse osmosis membrane and a synthetic emulsion using an Iranian crude oil has been employed. The flux-time curves have been analyzed using a modified form of Hermia's model to investigate the mechanism of flux decline. The results show that the experimental data is inconsistent with the Intermediate Blocking Filtration Model. Also, the limiting flux at all conditions has been determined.In this research, the results were evaluated using neural network modeling.

Keywords: Reverse osmosis membrane; Oil in water emulsion; Wastewater treatment, Artificial Neural Network

1. Introduction

Oily water emulsions are one of the main pollutants emitted into water by industry and domestic sewage. Also oily water in inland waterways and coastal zone has become one of the most serious issues of water pollution which needs to be resolved urgently [1-3]. So far, there exist several techniques for separation. Typical ones include chemical demulsification, pH adjustment, gravity settling, centrifugal settling, filter coalescer, heating treatment, electrostatic coalscers and membrane techniques, etc. [4-6]. There are some advantages and disadvantages to each of these demulsifications techniques. Traditional techniques used in the separation of unwanted oil-in-water (O/W) emulsions, such as gravity settlement (API separator), flow throw packed beds and air flotation have an important coalescence step. The efficiency of coalescing separators is dependent upon several factors, such as the droplet size distribution and the wettability of the media by dispersed phase. However, the inherent difficulty of dealing with biphasic flow makes the design and prediction of overall performance a difficult exercise. Applicability is also limited when surfactants are presented because they usually cause a radial slowdown in the coalescence. In these processes, using additives requires the use of a variety of chemicals including acid, iron and alumina sulphates, etc. The water phase from chemical treatment needs secondary purification to meet quality requirements for discharge system [7-9]. The pH effect can sometimes be used to break O/W emulsions, but the effect of pH and salts are not significant in water-in-oil (W/O) emulsions. Centrifugation is sometimes an efficient method for some emulsions; however its operating cost is fairly high to run and maintain. The competitive thermal process of oil removal requires large amount of energy [10]. The electric field method is also used but extremely high voltages (10-20KV) are required to cause droplet coalescence [11-13]. Investigation of the membrane separation processes for oily water treatment was started around 1973. The obvious advantages of membrane processes would be lower capital cost, the absence of chemical addition and subsequent generation of oily sludge. Concentrated oil from oily wastewater could be reused and handled with accumulated straight oils and, subsequently, disposed of into existing incinerators [14]. The target of this study is to find out the effect of operating conditions such as transmembrane pressure, cross flow velocity, temperature, oil concentration and salt concentration on flux and flux decline. The optimum operating conditions have been determined. In this study, it has been tried to determine the influence of temperature, transmembrane pressure and cross flow velocity on fouling and the effect of these parameters on permeate flux. Also, general models of fouling have been studied and model predictions have been compared with experimental data. The results of this study by use of ANN reflected a suitable accuracy.

2. Artificial Neural Network (ANN)

Recently, there have been a number of researches conducted on data processing for problems for which there is no solution, or problems that are not easily solvable. The ANN pattern is inspired by the neural system of living organisms that includes some constituent units called 'Neuron'. Most of the neurons are composed of the three main parts including cell body (that includes necluous and other protective parts), dendrites, and axon. The last two parts are the communicative parts of the neuron. Figure 1 displays the structure of a neuron.

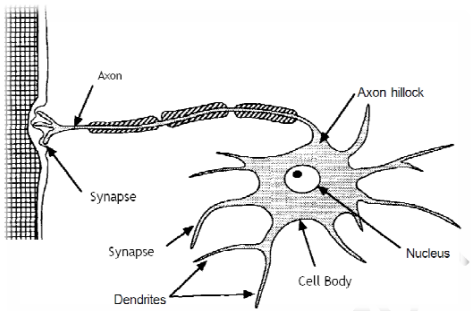

Figure 1. *Major parts of a biological cell*

Dendrites, as electric signal receiving areas, are composed of cell fybers with unsmooth surface and many splitted extensions. That is why they are called tree-like receiving networks. The dendrites transfer the electrical signals into

cell nucleous. The cell body provides the required energy for neuron activity that can be easily modeled through an addition and comparison with threshold level. Unlike Dendrites, axon has a smoother surface and fewer extensions. Axon is longer and transfers the received electro-chemical signal from the cell nucluous to other neurons. The cinfluence of a cell's axon and dendrites is called synapse. Synapses are small functional structural units that enable the communication among neurons. Synapses have different types, from which one of the most important ones is the chemical synanpse. Artificial neural cell is a mathematical equation in which p represents an input signal. After strengthening or weakening as much as a parameter w (in mathematical terms, it is called weight parameter), an electric signal with a value of pw will enter the neuron. In order to simplify the mathematical equation, it is assumed that the input signal is added to another signal with b value in the nucluous. Before getting out of the cell, the final signal with a value of $pw + b$ will undergo another process that is called "Transfer function" in technical terms. This operation is displayed as a box in Figure 2 on which f is written. The input of this box is the $pw + b$ signal and the output is displayed by a. mathematically, we will have:

$$a = f(pw + b)$$

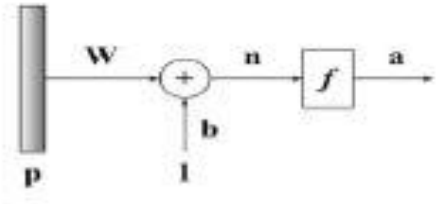

Figure 2. *Mathematical model of a neuron*

Putting together a great number of the above-mentioned cells brings about a big neural network. As a result, the network developer must assign values for a huge number of w and b parameters; this process is called learning process. Within the structure of neural networks, sometimes it is needed to stack up a number of neurons in a layer. Moreover, it is possible to take advantage of neuron crowds in different layers to increase the system efficiency. In this situation, the network will be designed with a certain number of inputs and outputs too; while the difference is that there would be more than one layer (instead of having only one layer). In this manner (multi-layer network), the input layer is the layer through which the inputs are given to the system, the output layer is the layer in which the desired the results are delivered, and the other layers are called hidden layer. Figure 3 displays a neural network with three layers. Input layer, output layer, and hidden layer (that is only one layer in this figure). Through changing the number of hidden layers, and changing the number of present neurons in each layer, it is possible to enhance the network capabilities.

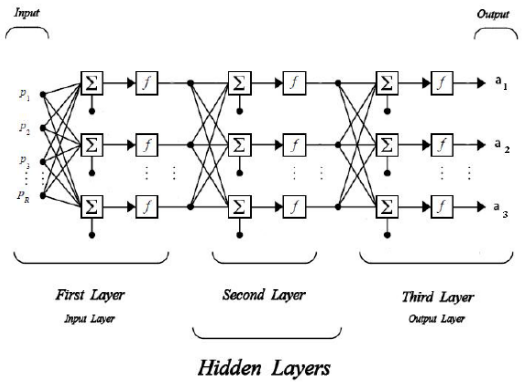

Figure 3. *A schematic view of Neural Network and its constituent layers*

2.1. Modeling of hydrogenation process by use of Neural Network

In this research, the influence of ANN input parameters (operation condition) on the efficiency of conversion hydrogenation. One ANN was designed for analysis of the conversion parameter. Feed-forward multilayer perceptron ANN and Levenberg-Marquardt function with two inputs and two outputs were used. The Tansig transfer function was used for the hidden layer, and Purelin was utilized for the output layer. Five neurons were determined for the hidden layer. After data processing, 70 percent was dedicated for learning, 30 percent was dedicated for testing. Such organic compounds as ethanol was selected in this research; and, Matlab version R2014b was used. Figure 4 displays a schematic view of a two-layer ANN with only one hidden and output layer.

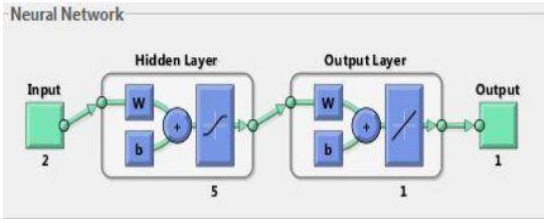

Figure 4. *A schematic view of the ANN*

The inputs are multiplied by a w value, and there is a bias factor (b) that is added to the input (bias is a fixed value that is added to the input in order to increase the accuracy). Afterward, the result will undergo a function and the resulted value will be multiplied by a weight and added with a bias. The final result will pass another function (with different form and functionality) and output is made. There are five neurons and two inputs on the first layer; however, the number of neurons in the output layer is the same as the number of outputs. The following points about the algorithms must be considered:

The Data Division compartment totally scrambles the defined data for the system. This compartment randomly defines the Train, Validation, and Test data, so that there will be samples from everywhere of the environment.

Levenberg-Marquardt function was used in Training phase.

The Mean Squared Error (MSE) functions for performance measurement.

The default settings were used for derivative issue.

Epoch is accepted from iteration 0 to 1000. It means the weights consecutively changed for 1000 times based on the Levenberg-Marquardt function, and the training procedure was done. If the iteration number reaches 1000, the procedure stops (here it stopped at 24). There was no limit for time (but it could be set for training to stop after 30 seconds for example). Validation check is the maximum number of times that network failure can be tolerated (figs 5 and 6).

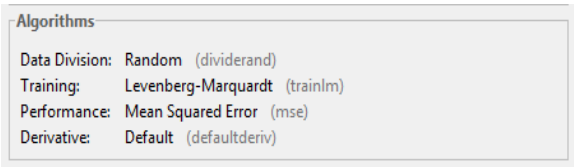

Figure 5. *Algorithms compartment in ANN*

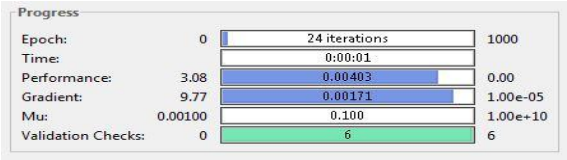

Figure 6. *Graph of Validation check of network*

3. Materials and Methods

FilmTec polyamide FT30 reverse osmosis membrane was used for all experiments. The experimental setup is shown schematically in Figure 7.

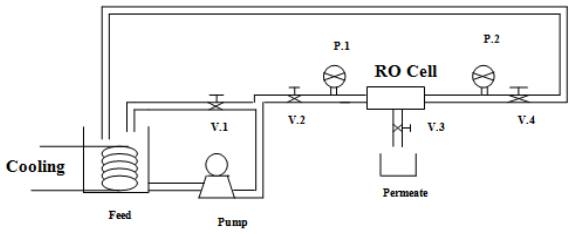

Fig 7: *Scheme of RO crosses flow system*

3.1. Experimental Setup

The experimental setup is shown schematically in Figure 7. Feed, which is a synthetic emulsion made by blending the organic phase containing an Iranian crude oil with distilled water was pumped by means of a centrifugal pump into the module. The membrane cell is a flat type module having a basin with 150 mm length, 60 mm width and 3 mm depth. The effective area was 90 cm2. It is composed of two separate parts made of stainless steel and has two outlets in order to pass the feed on the membrane surface. Support is put between these two parts in order to mechanically protect the membrane against operational pressure. FILM TEC polyamide FT30 membrane was employed for all experiments.

3.2. Operating Conditions

The transmembrane pressure was adjusted by the throttling valves V2 and V4 between 7 and 15.5 barg. The feed temperature was varied between 20 and 50 °C by means of a small heat exchanger into the feed tank. Permeate collected in a sample bottle was measured and then recycled to the feed tank. The inlet and outlet flow pressure of the cell was read from two pressure gauges and average value of these two data was considered as the operational pressure. Transmembrane pressure can be calculated using the following equation:

$$\Delta P_{av} = \frac{(P_i - P_o)}{2} - P_p \quad (1)$$

Where Pi and Po are inlet and outlet pressures, respectively and Pp is permeate pressure which is atmospheric. The outlet flow of the cell can be led out of the system or returned to the tank. The permeate of membrane can be collected in another tank. Volume of feed was about 9 lit but volume of permeate was about 50 ml after 1-2 hr.

3.3. Evaluation Method

The permeate flux through the cake layer and membrane is calculated according to Darcy's law [13]:

$$J = \frac{\Delta p}{\mu \sum R} \quad (2)$$

Where Δp is the transmembrane pressure imposed to the membrane system as a driving force, μ is fluid viscosity and ΣR is all resistances in the permeation path. Each membrane has a special unique resistance, which depends on its pore size and its thickness. This resistance known as Rm can be calculated using initial flux of distilled water (Jwi) according to the following equation:

$$R_m = \frac{\Delta p}{\mu . J_{wi}} \quad (3)$$

The resistance observed after feed filtration could be calculated using flux of distilled water after fouling and washing with water (Jww). This resistance is known as Rf and is calculated using the following equation:

$$R_f = (\frac{\Delta p}{\mu . J_{ww}}) - R_m \quad (4)$$

Rjection coefficient can be calculated using the following equation:

Efficiency = ((C1-C2)/C1)*100 (5)

Where C1 and C2 are oil concentrations in the feed and permeate respectively. The oil concentration in permeate was determined by using NDIR Analyzer of Hydrocarbon in water-Horoba, Japan, Model OCMA310.

4. Results and Discussion

4.1. Effect of transmembrane pressure

Effect of transmembrane pressure on permeation flux of water at a temperature of 20°C and a concentration of 0.3 ~01% is presented in Fig. 8. As can be observed, permeation flux increases with increasing transmembrane pressure. It can be explained that the higher transmembrane pressure results in droplets to pass rapidly through the membrane pores. As shown, permeation flux initially decreases with time; however the flux gradually reaches to a constant value

depending on transmembrane pressure. This is due to membrane fouling.

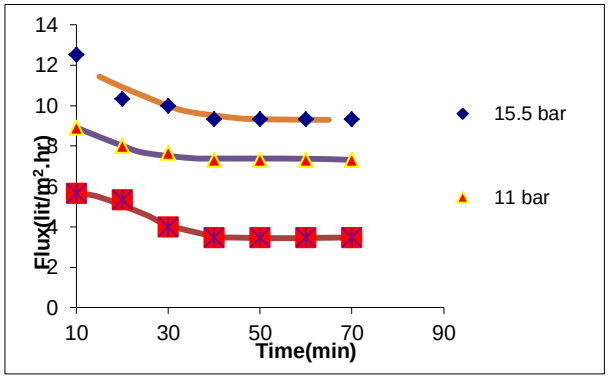

Fig 8: *Effect of transmembrane pressure on permeation flux (Experimental Data and Network Model Data)*

Temperature and cross flow velocity were kept constant for all pressures at 20 °C and 1 m/sec, respectively, while oil concentration was 0.3% Vol. As can be seen from the figures 8 and 9, the neural network model predicts well the experimental results.

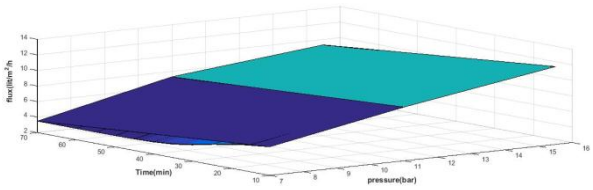

Fig 9: *Network Model Prediction for effect of troansmembrane pressure on permeation flux*

4.2. Effect of Oil Concentration

Fig. 10 shows the effect of oil concentration on membrane fouling. All experiments have been carried out at a temperature of 20°C and a pressure of 13 bar.

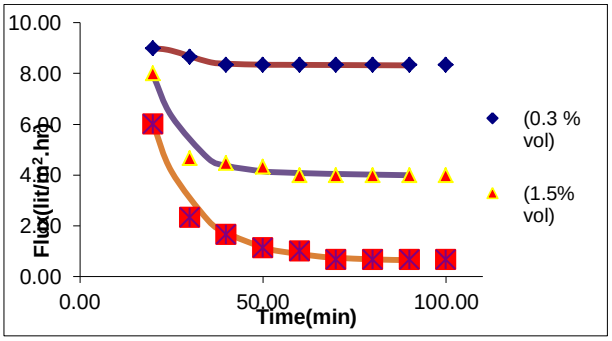

Fig 10: *Effect of oil concentration on permeation flux (Experimental Data and Network Model Data)*

The results show that permeation fluxes of higher oil concentrations decrease steeper at early filtration times. At higher concentrations, the flux decline is the same and flux reaches a constant value almost independent of oil concentration. This is due to the fact that at higher concentrations, fouling is not affected by oil concentration. As can be seen from the figures 10 and 11, the neural network model predicts well the experimental results.

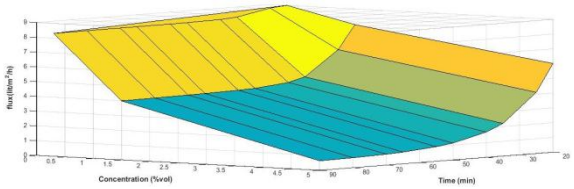

Fig 11: *Network Model Prediction for Effect of oil concentration on permeation flux*

4.3. Effect of Cross Flow Velocity

To study the effect of cross flow velocity on fouling, some experiments have been carried out within a cross flow velocity range of 0.95-l .55 ms-‘. As shown in Fig. 12, increasing cross flow velocity leads to an increase of turbulency and mass transfer coefficient weakens the effect of polarization and increases the permeation flux.

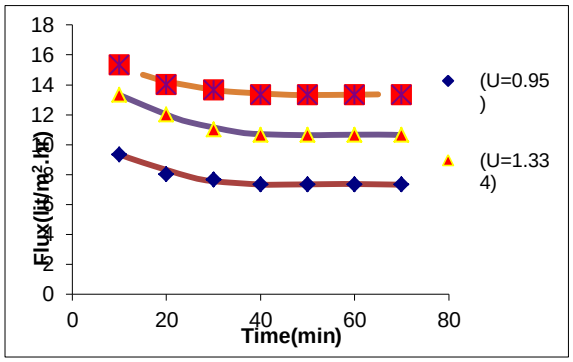

Fig 12: *Effect of cross flow velocity on permeation flux (Experimental Data and Network Model Data)*

It must be mentioned that all experiments have been carried out at a concentration of 0.3 vol%, a pressure of 13 bar and a temperature of 20°C. As can be seen from the figures 12 and 13, the neural network model predicts well the experimental results.

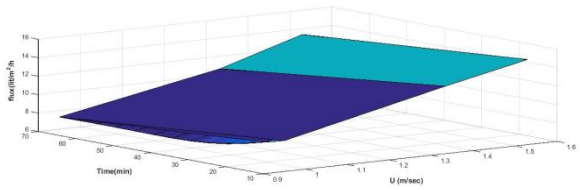

Fig 13: *Network Model Prediction for Effect of cross flow velocity on permeation flux*

4.4. Effect of Temperature

According to the emulsion stability, temperature has been found to be an important factor, As shown in Fig. 14, permeation flux increases significantly when temperature changes 20-50°C.

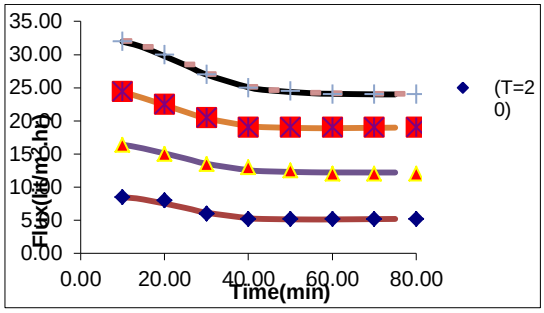

Fig 14: *Effect of feed temperature on permeation flux (Experimental Data and Network Model Data)*

Increasing temperature causes an increase in viscosity reduction. It can be explained by the fact that viscosity reduction in this temperature range is responsible for the flux improvements. It must be mentioned that The transmembrane pressure and cross flow velocity were keep constant for all temperatures at 13 bar and 1 m/sec respectively, while oil concentration was 0. 3% Vol. As can be seen from the figures 14 and 15, the neural network model predicts well the experimental results.

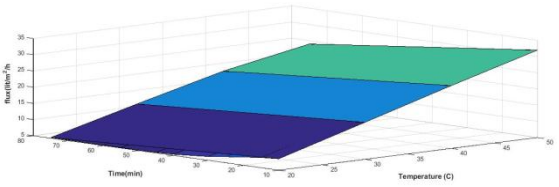

Fig 15: *Network Model Prediction for Effect of feed temperature on permeation flux*

5. Conclusion

From the results, the following conclusions can be drived:

- Increasing Pressure increases flux but decreases oil rejection.
- Increasing cross flow velocity increases flux.
- Increasing temperature increases flux linearly, however, higher temperatures may damage the membrane
- Also, the results of reverse osmosis membrane tests were compared with neural network modeling and showed that neural network model predicts well experimental results.

References

[1]. M. Rabiller-Baudry, L. Paugam, L. Begoin, D. Delauney, M. Fernandez-Cruz, C. Phina-Ziebin, C. L-G. Guadiana, B. Chaufer, Alkaline cleaning of PES membranes used in skimmed milk ultrafiltration: from reactor to spiral-wound module via a plate-and-frame module, Desalination, 191, 334-343, 2006.

[2]. V. B. Briao, C. R. G. Tavares, Pore blocking mechanism for the recovery of milk solids from dairy wastewaters by ultrafiltration, Brazilian Journal of Chemical Engineering, 29, 93-407, 2012.

[3]. M. Kazemimoghadam, T. Mohammadi, Chemical cleaning of ultrafiltration membranes in milk industry, Desalination, 204, 213-218, 2007.

[4]. M. A. Razavi, A. Mortazavi, M. Mousavi, Dynamic modeling of milk ultrafiltration by artificial neural network, Journal of Membrane Science, 220, 47-58, 2003.

[5]. X. T. Jimenez, A. A. Cuenca, A. T. Jurado, A. A. Corona, C. R. M. Urista, Traditional methods for whey protein isolation and concentration: effects on nutritional properties and biological activity, Journal of the Mexican Chemical Society, 56, 369-377, 2012.

[6]. M-J. Corbaton-Baguena, M-C. Vincent-Vela, S. Alvarez-Blanco, J. Lora-Garcia, Analysis of two ultrafiltration fouling models and estimation of model parameters as a function of operational conditions, Transport in Porous Media, 99, 391-411, 2013.

[7]. M. Rezakazemi, S. Shirazian, S. N. Ashrafizadeh, Simulation of ammonia removal from industrial wastewater streams by means of a hollow-fiber membrane contactor, Desalination, 285, 383-392, 2012.

[8]. G. Bolton, D. LaCasse, R. Kuriyel, Combined models of membrane fouling: development and application to microfiltration and ultrafiltration of biological fluids, Journal of Membrane Science, 277, 75-84, 2006.

[9]. P. Aimar, S. Baklouti, V. Sanchez, Membrane-solute interactions: influence on pure solvent transfer during ultrafiltration, Journal of Membrane Science, 29, 207-224, 1986.

[10]. P. Schausberger, N. Norazman, H. Li, V. Chen, A. Friedl, Simulation of protein ultrafiltration using CFD: comparison of concentration polarization and fouling effects with filtration and protein adsorption experiments, Journal of Membrane Science, 337, 1-8, 2009.

[11]. B. Marcos, C. Moresoli, J. Skorepova, B. Vaughan, CFD modeling of a transient hollow fiber ultrafiltration system for protein concentration, Journal of Membrane Science, 337, 136-144, 2009.

[12]. H. Rezaei, F. Z. Ashtiani, A. Fouladitajar, Fouling behavior and performance of microfiltration membranes for whey treatment in steady and unsteady-state conditions, Brazilian Journal of Chemical Engineering, 31, 503-518, 2014.

[13]. J. Hermia, Constant pressure blocking filtration laws: application to power-law non-Newtonian fluids, Chemical Engineering Research and Design, 60, 183-187, 1982.

[14]. D. Mignard, D. H. Glass, Fouling during the cross-flow ultrafiltration of proteins: a mass-transfer model, Journal of Membrane Science, 186, 133-143, 2001.